ANALYSIS OF APPROXIMATED CURVED CRACKS IN HOMOGENEOUS AND GRADED MATERIALS

HAYDER FANOOS NEAMAH
Mechanical Engg. Dept., Baghdad University,

ABSTRACT

In this paper two stages of analysis are studied. In stage I, the influence of crack shape on the crack-tip stresses, critical loads and subsequent propagation direction is investigated via a simple analytical model for cracks in homogeneous materials. This model is verified through finite element simulations using ANSYS. It is demonstrated that accurate predictions of mechanical energy release rate and crack deflection angle may be obtained from a smaller number of crack shape parameters.

In stage II, this concept is extended to curved cracks in functionally graded materials (FGMs).It is common that analytical and computational models of fracture in FGMs have focused almost extensively on straight cracks. If it can be demonstrated that straight cracks give an adequate approximation of curved cracks in graded materials, then the existing solutions for straight cracks provide a sufficient foundation for fracture analysis of FGMs. On the other hand, if straight cracks do not adequately approximate curved cracks in FGMs, then the development of solutions for non straight cracks in graded materials is priority. Three cracks shapes approximations are performed to compare with the actual crack in isotropic and graded materials. The crack propagation and the SIFs were simulated using finite element method. It was concluded that piecewise linear crack shapes provide a significantly better approximation than straight crack shapes. Accordingly, analytical solutions for piecewise linear cracks in graded materials would be very useful, and should be a focus of future work in this area.

KEY WORDS
SIF, FGM, Fracture mechanics, FEA, ANSYS

الخلاصة:

في هذا البحث تم دراسة مرحلتين من التحليل. في المرحلة الاولى , دُرس تحليلياً تأثير شكل الكسر على اجهادات القمة عند الكسر في المواد المتجانسة. وتم الحصول على نتائج مقاربة من خلال أستخدام برنامج العناصر المحددة ANSYS . في المرحلة الثانية هذا التحليل توسع لدراسة تأثير شكل الكسر في المواد الطبقية . من الشائع في النموذج الحسابي و النظري للكسر في المواد الطبقية(المتدرجة في معامل المرونة) استخدام الكسر الخطي لتمثيله. اذا تم اثبات انه الكسر الخطي يعطي نتائج تقريبية للكسر الحقيقي ,فان الحلول المتوفرة

للكسر الخطي تعطي صورة كافية للكسر الحقيقي. اما اذا ثبت العكس فانه الكسور اللخطية هي الاساس في التحليل. ثلاثة اشكال تقريبية من الكسر تم أستقصاؤها لمقارنة الاجهادات عند القمه لمواد متجانسة ومواد طبقية . أنتشار الكسر والمقارنة تمت باستخدام العناصر المحددة. لوحظ أنه شكل الكسر الخطي المتدرج يعطي نتائج تقريبية من الاشكال التقريبية الاخرى بالمقارنة مع الشكل الحقيقي للكسر. وعليه الدراسة النظرية للكسر الخطي المتدرج في المواد الطبقية هي الاكثر صحة لدراسة ميكانيك الكسر في المواد الطبقية.

INTRODUCTION

FGMs (functionally graded materials) are "functionally graded" to provide the exact combination of characteristics desired, and in these materials or structures the material properties vary with location in such a way as to optimize some function of the overall FGM. The metal, the ceramic, the volume, shape, location of the ceramic, and the fabrication method can all be tailored to achieve particular desired properties. The design of FGMs requires an explicit understanding of the material behavior at each location and over all these length scales. There has been quite considerable work on the manufacturing methods of metal/ceramic FGMs. Advanced manufacturing techniques are used to process FGMs, among which we may mention spark plasma sintering (SPS), 3D-printing, electrophoretic deposition and high–temperature infiltration (Jin et al., 2001). Due to the brittle nature of the ceramic components in ceramic/metal FGMs, fracture mechanics of graded materials is also studied quite extensively. A detailed literature review of the fracture mechanics of graded materials is given by Dag (2004). Functionally graded microstructure in a ceramic/metal composite has been found to reduce the otherwise thermal stress field at the interface between ceramic and metal plates(Taya et al., 2005). Chatterjee et al. (2006) have developed a multi-layered rainbow type actuator with graded piezoelectric properties through the thickness.

The criteria for crack propagation should take into consideration the account of the influences of material property gradient along with crack geometry and applied loading, on the applied stress intensity factor (Erdogan, 2006). Furthermore, it should be include the effects of intrinsic toughness variation (Jin & Batra, 2007). Although a crack shape may be quite complicated, several researches have suggested that the stress intensity factor may be approximated by a function of several simple crack-shape parameters, or indeed by approximating the curved crack to an equivalent straight crack. The relevance of these types of approximation has been demonstrated for particular crack-shapes and loading configurations, although reasons were not given for why this is so (Kitagawa et al.,1975, Leevers et al., 1980, Noda et al., 1994). Approximations to an equivalent straight crack, or other simplified crack-shape, simplifies calculation appreciably and may often sufficiently accurate. In fact, this approximation is made when treating any macroscopically straight crack as being perfectly straight, despite the fairly ubiquitous presence of crack deflection at a microscopic level. The validity of the approximation in this case is generally not questioned. For macroscopically deflecting cracks, this approximation is clearly useful for simply estimating fracture parameters, and thus warrants further investigation.

It is proposed that the shape of a crack may be described by several parameters, from which an approximate SIF value may be predicted. For an edge crack, a common configuration in experiment fracture mechanics, the proposed parameters, shown in Fig. 1. are:

- Crack length perpendicular to the edge, a;
- Transverse deviation parallel to the edge, d;
- Crack-tip orientation relative to loading direction, ϕ.

In this paper, the influence of crack shape on crack tip stresses in homogeneous materials is investigated via a simple analytical model. This model is verified through finite element simulations. Second, the curved cracks of graded materials were simulated by FE program ANSYS.

MATERIALS AND METHODS

Analytical Model(For Homogeneous Material)

A simplified approach given by Ashby and Jones (1996), for calculating the mechanical energy release rate, based on the assumption of an elliptical region of stress relaxation around the crack and the increase in this region with the crack extension. For a straight crack of length, 2a, as in Fig.2, the rate of energy release, G, associated with a crack extension was determined as:

$$G = \frac{k\pi\sigma^2 a}{2E'} \tag{1}$$

Where E' is the effective Young's modulus, and k describes the aspect ratio of the relaxation volume. It can be shown that k is 2, for a through-thickness straight crack in an infinite medium.

Mechanical Energy Release Rate

The mechanical energy release rate is calculated from the following formula (Noda et al., 1994):

$$G = \frac{\pi\gamma\sigma^2}{4E'}[2a(\cos\eta + d\sin\eta)\cos(\phi - \eta)] \tag{2}$$

To estimate the value of γ, the simple case of a straight crack under tensile loading is considered. In this case, parameter d, θ and η are zero, and:

$$G = \frac{\pi\gamma\sigma^2 a}{2E'} \tag{3}$$

This may be compared with the known expression for an edge crack (Broek, 1991):

$$G = \frac{1.12^2\pi\sigma^2 a}{E'} \tag{4}$$

And the geometrical constant is thus determined as $\gamma = 2(1.12)^2 \approx 2.5$.

Deflection Angle

Whilst a number of different criteria have been used to predict deflection angle, the focus of the current analysis is strain energy release rate. Accordingly, the maximum energy release rate criterion is most appropriate. Considering a kink extending at angle from the tip of a particular curved crack the mechanical energy release rate is estimated from Eq. (2) as:

$$G(\theta) = \frac{\pi\gamma\sigma^2}{4E'}[2a(\cos\eta + d\sin\eta)\cos(\phi - \eta + \theta)] \tag{5}$$

This is maximized for:

$$\frac{dG(\theta)}{d\theta} = 0 \tag{6}$$

After simple sequence of calculations, the optimum value of the kink angle, :

$$\theta_k = \eta - \theta \tag{7}$$

This implies that mechanical energy release rate will be maximized for crack growth perpendicular to the loading direction, which is understood to be the case.
This simple analytical model may not be applied to FGMs, as the elastic property gradient, leads to a spatial variation in strain energy density. It was assumed, however, that curved cracks in FGMs, by analogy with those in homogeneous materials, may also be approximated by simple-shaped cracks. This was investigated with FE simulation, using several different crack-shape approximations.

FINITE ELEMENT SIMULATIONS (FOR BOTH FGMS AND HOMOGENEOUS MATERIALS)

Geometric Modeling

Specimens were modeled in two dimensions under plane stress conditions. Generally, compositionally symmetrical samples, consisting of two graded sections situated between materials 1 and 2, as in Fig. 2. A tensile load is applied to the edge of the plate and the other is clamped. Crack propagation was assumed to initiate from a notch in the graded section, oriented perpendicular to the gradient section. The material gradient was described by the magnitude of elastic property mismatch, $R_E=E_2/E_1$, the width, w, and the shape of the elastic property profile, defined by the exponent, n, in a power-law expression. Continuous and stepped gradients respectively, as shown in Fig. 3, were defined by

$$E(\xi) = E_1(1+(R_E-1)\xi^n) \quad \text{(Continuous)} \tag{8}$$

$$E(\xi) = E_1(1+(R_E-1)(Int[N_s\xi]/N_s)^n) \quad \text{(Stepped)} \tag{9}$$

Where N_s is the number of steps across the gradient and $Int[N_s\xi]$represents the operation of rounding to the nearest integer. Stepped gradients with smoothing of effective properties at step interfaces were also considered.

In linear elastic problems, it is known that the displacements near the crack tip (or crack front) vary as $\sqrt{r}$, where r is the distance from the crack tip. The stresses and strains are singular at the crack tip, varying as $1/\sqrt{r}$. To resolve the singularity in strain, the crack faces should be coincident, and the elements around the crack tip (or crack front) should be quadratic, with the midside nodes placed at the quarter points. Such elements are called singular elements. Fig. shows 2D singular element. Meshing was conducted under free meshing conditions using the AMESH command, with isoparametric quadrilateral PLANE 82 elements which have 8 nodes: 4 vortex nodes and 4 midside nodes. The crack tip singularity were modeled using degenerate triangular quarter point elements, which enabled crack tip fields and fracture parameters to obtained. An example of meshing is given in Fig. 4. To improve solution accuracy, the mesh was refined around the crack and the crack tip in particular, with crack tip element size ($a_o/1000$) where a_o is initial crack length, as shown in Fig. 3. approximately 3500 elements were used in total.

Simulation Of Crack Propagation

Crack propagation was simulated incrementally. Fig. 5 shows a schematic diagram explaining the sequence of events in simulation of crack propagation.

SUMMARY

These were conducted in two stages. In stage I, stationary cracks with a range of shapes in homogeneous specimens were modeled to obtain values for mechanical energy release rate and deflection angle. In stage II, propagation of cracks in homogeneous and graded specimens was simulated, and crack paths and SIF profiles were obtained.

The general specimen configuration for stage I, an edge-cracked size with stresses applied to edge of plate, and a representative mesh, are shown in Fig. 4. Deflection angle was predicting using the maximum energy release rate criterion for consistency with the analytical model.

To investigate a range of crack shapes, a degree of variability within the constraints of the set parameter scheme was introduced by varying the curvature of the cracks, whilst keeping the defined parameters constant. Three different general crack shapes were considered, A, B and C, as shown in Fig. 6. By using each of these for each set of values of a, d, and, the sensitivity to curvature could be examined. It should be noted that, in the geometrical scheme used, the radius of curvature, r, is proportional to a and d, so that when d is varied, the relative curvature, i.e. r/a varies also.

When the entire crack shape was used, the finite extension per increment resulted in a path made up of numerous small line segments. As the propagation direction did not change abruptly, these formed a smooth path. The effect of using approximated crack shapes on predictions of crack-path and stress concentrations was examined. When simplified crack-shapes, as shown in Fig. 7(a), were used, the crack was extended in the same way; however, after each crack extension, a new approximated crack-shape was defined and meshed. This approximated crack shape was used for calculation of the propagation direction for the subsequent increment. This is illustrated schematically in Fig. 7(b). The crack-shape geometry and surrounding mesh was deleted and refined between each increment of the propagation. The crack paths presented here are essentially plots of the variation of crack-tip location, as calculated using a variety of crack-shape approximations.

It should be emphasized that the use of approximated crack shapes in this manner did not improve simulation efficiency, except for simplifying the mesh pattern around the crack which could slightly reduce the number of elements and hence the computation time. Rather, the efficiency of analytical solutions would be improved notably if a simplified crack shape could be used. Establishing the validity of this was a principal aim of this study.

This approach was applied to several different material configurations. The general specimen geometry, an edge-cracked plate in tension, is depicted in Fig. 3. Specimens containing the following material interface configurations were examined:

(1) No interface (asymmetrically-notched homogeneous specimen), with the notch situated 36 mm from the load line (center of specimen).
(2) Step interface (biomaterial specimen), with crack initially 8 mm from the interface;
(3) Continuously-graded interfaces, with parabolic spatial variation in material properties across a 10 mm wide gradient region, and crack initially situated 8 mm from the interface between the gradient region and material 1;
(4) Continuously graded interface, with parabolic spatial variation in material properties across a 10 mm in wide gradient region, and crack initially situated 8 mm from the interface between the gradient region and material 1;
(5) Discontinuously-graded interface, with stepped-linear (3 steps) spatial variation in material properties across a 10 mm wide gradient region, and crack initially situated 8 mm from the interface between the gradient region and material 1.

The assumed properties of material 1 were $E_1=3.4, v_1= 0.25$. Properties of material 2 were assumed as $E_2=340$ and $v_2=0.25$ for all cases except the homogeneous specimen, which material 1 and 2 were identical (Mattew T.Tillbrook, 2005). The large disparity in elastic properties was assumed so that deflection angles would be high, thereby amplifying the differences which may arise between predictions from different crack-shape approximations.

RESULTS & DISCUSSION

Curved Cracks In Homogeneous Materials

The predictions from this analytical model are shown in Figures 8 to 10, along with results obtained from finite element analysis. The FE results are shown as dots or triangles, with a degree of scatter between results obtained for different shape types, A, B and C, whilst analytical model results are shown as solid lines. Mechanical energy release rate values are normalized with respect to effective Young's modulus, E', and applied stress, σ , so that the effect of crack geometry may be examined directly. However, as applied stress and effective Young's modulus were held constant for all cases examined, the absolute and normalized values for mechanical energy release rate are directly proportional.

The effect of variation in relative deviation, d, is illustrated in Figs.8a and b for cracks with loading angles of $\eta = 0^0$ & 30^0 respectively. There is a systematic influence of d on the deflection angle. Although the difference is larger for larger values of d, the influence of d seems to be greater for smaller d values, as the slope of the variation of θ with d is greater in that region. Variation in d leads to a variation in the curvature at the crack tip, so the influence of d is likely to be attributable to curvature.

The effect of variation in crack-tip angle, ϕ , is illustrated in Fig. 9(a and b) for cracks with loading angles of $\eta = 0^0$ & 30^0 respectively. Crack-tip orientation is seen to influence fracture parameters significantly. Increasing the crack-tip angles leads to an increase in deflection angle, and a decrease in mechanical energy release rate. Very close agreement is observed between the model and FE predictions for both energy release rate and deflection angle.

The effect of variation in crack shape is illustrated in Fig.10 (a and b) for cracks with loading angle of $\eta = 0^0$ & 30^0 respectively. In these cases, the key shape parameters remain constant whilst the shape of the crack is varied. This was achieved by varying the radius of curvature in the circular arc section of the crack shape. Crack curvature has only a minor influence on fracture parameters, as anticipated in the original hypothesis. This implies that a wide range of cracks may be simulated reasonably accurately by analogy with simplified crack shapes. Crack curvature does seem to have a slight effect, especially when the radius of curvature near the crack tip is small. This is in agreement with the findings of (Kitagawa et al., 1975).

Curved Crack In Graded Materials

Crack paths and SIF magnitude profiles obtained using each of the approximated crack shapes are compared with these obtained using the entire crack-path shape, in Figs 11 to 15. SIF magnitude has been normalized with respect to the SIF for straight crack of the same length in a homogeneous specimen of the same dimensions and loading. This allows the influence of material property variation to be examined independent of the effects of crack length, which would otherwise dominate the variation of SIF magnitude. The normalized SIF magnitude profiles are plotted against crack-tip position in the horizontal direction so that variation across the interface region may be compared between the different crack-shape approximations.

Fig. 11 shows results for the asymmetrically-notched homogeneous specimen. Path predictions and SIF magnitudes obtained using crack-shape approximations show very good agreement with those obtained using the entire crack-path. In the homogeneous material specimen in Fig.11, the use of an approximated crack shape appears to have almost no effect at all on SIF magnitude predictions. Results for the bimaterial specimen are presented in Fig. 12. Deviation between results from approximated crack shapes and the entire crack path is more significant in this case. Fig. 12 and 14 show the results for the two continuously graded specimens with different gradient steepness. Results for the discontinuously graded (step graded) specimen, which contained three steps, are shown in Fig. 15.

The presence of material inhomogeneity, in Figs 12 to 15, seems to cause greater deviations between results from approximated crack shapes and those obtained using the entire crack path. In

inhomogeneous specimens, the results predicted using straight deviated significantly from the results for exact crack shape. Those approximations tended to result in less deflection. This could be attributed to a slight skewing of the crack tip stress field, caused by the difference in crack tip orientation of the approximated and exact crack shapes. The piecewise linear approximation gave good predictions for all the configurations examined.

The crack path shows a cumulative deviation effect. In the first increments of crack growth, before any deflection has occurred, the exact and approximated crack shapes are identical, and then they become progressively more different as the crack propagate, as was shown schematically in Fig. 7(b). Concordant with this, differences in the crack propagation direction, due to the use of a crack shape approximation, are initially very small then these increase as the crack extends. Furthermore, the differences accumulate, and the differences between crack paths lead to further divergence.

For cracks in the specimen with some material inhomogeneity, the SIF magnitude varied significantly across the interface region. In Fig. 12, it increases sharply as the biomaterial interface is approached. A similar effect is observed as the crack approaches the two interfaces in the step graded specimen in Fig. 15. A more continuous variation in SIF magnitude is observed for the continuously graded specimens, though these still exhibit notable variation with crack tip position. The contrast between the results for linear property variation in Fig. 13 and those for parabolic variation in Fig. 14 highlights the importance of material property distribution in influencing crack tip stresses.

For the crack approaching the biomaterial interface in Fig. 12, SIF magnitudes varied significantly between simulations using different crack shape approximations. For a crack with tip situated 1 mm from the bimaterial interface, for instance, the relative SIF magnitude calculated for using exact crack shape is 1.8 times that calculated using the straight crack approximation. This means that using the straight crack approximation would lead to an overestimate of critical load by a factor of 1.8. Similar comparisons may be made for crack in continuously graded and step graded specimens. These also show significant differences between SIF magnitudes obtained from different crack shape approximations.

CONCLUSIONS

From this analysis, the following concluding points can be deduced,

1. Curved cracks in homogeneous materials may be reasonably approximated by equivalent straight cracks for the calculation of mechanical energy release rates and deflection angles.
2. Piecewise linear crack shapes provide a significantly better approximation than straight crack shapes. Accordingly, analytical solutions for piecewise linear cracks in graded materials would be very useful, and should be a focus of further work in this area.

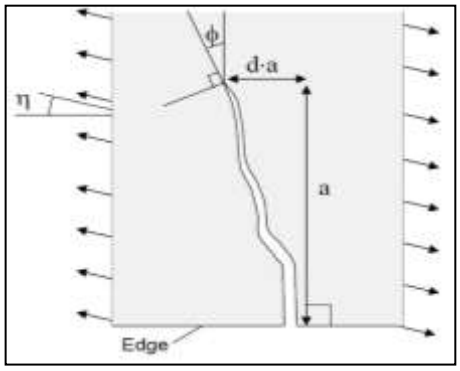

Fig. 1 Example of deviating crack showing key parameters

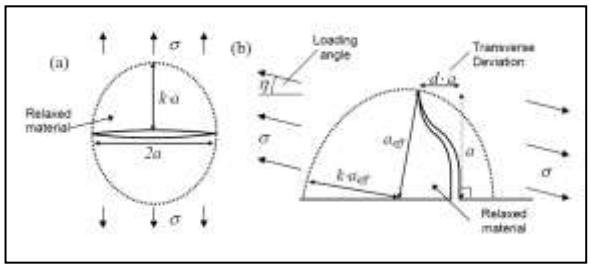

Fig. 2 Stress relaxation volume around (a) a straight internal crack under tensile loading (b) a curved edge crack under mixed mode loading

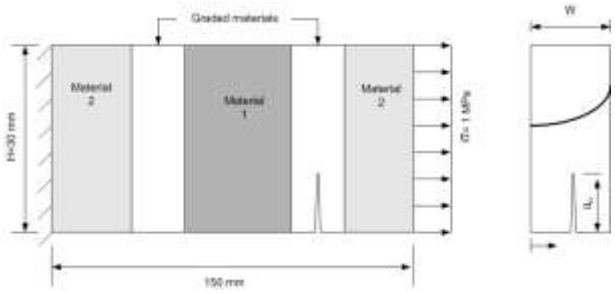

Fig. 3 Graded material specimen used in simulation

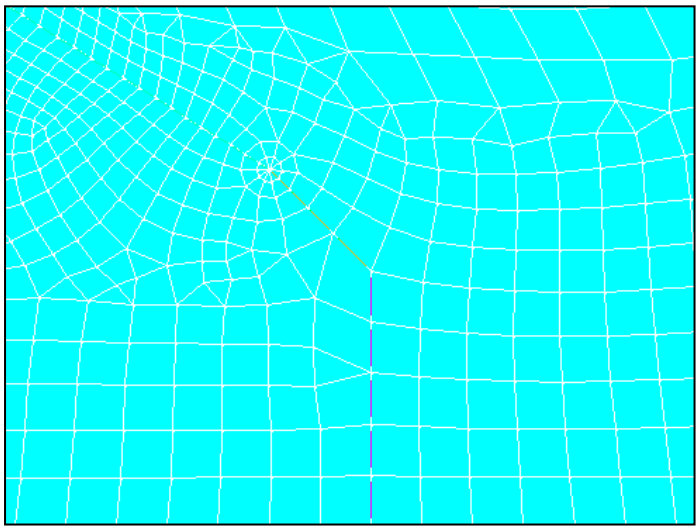

Fig. 4 Representative meshing of finite element modeling around the crack tip and crack front

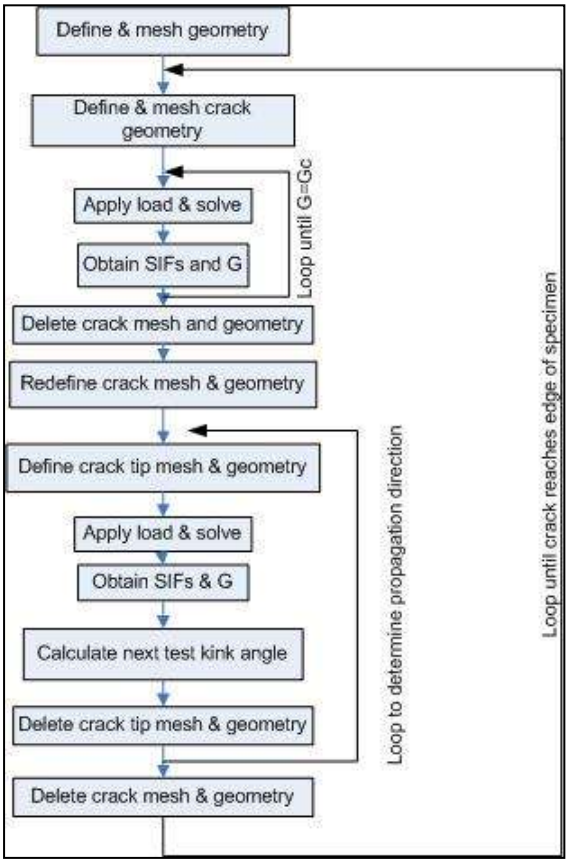

Fig. 5 schematic diagram shows the sequence of procedure of crack propagation using ANSYS

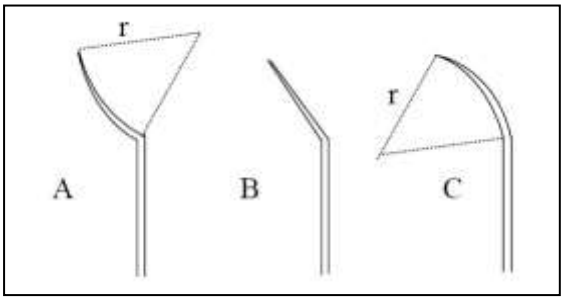

Fig. 6 Generic crack shapes used in FE validation (Stage I):A-Concave, B-Piecewise linear, C-Convex(Stage I)

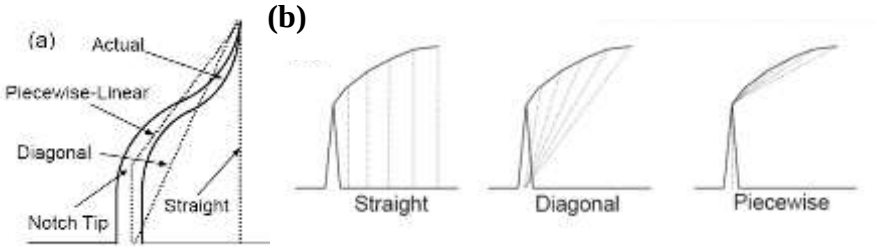

Fig. 7 Illustration of crack approximation (Stage II)

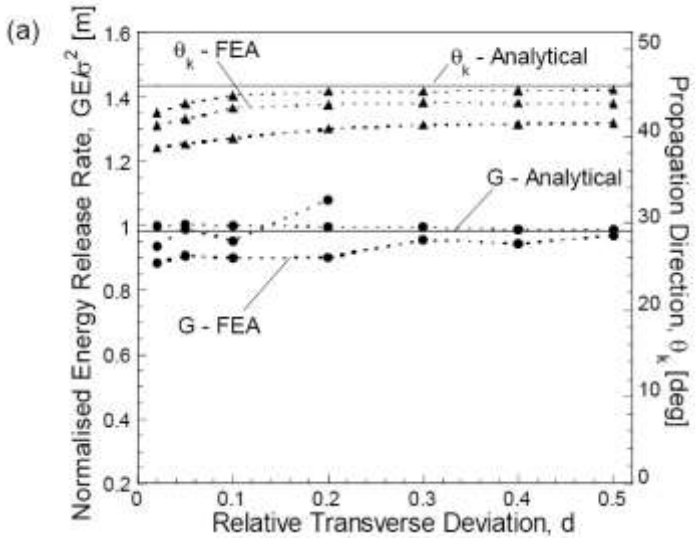

Fig. 8a Effect of transverse deviation, d, on mechanical energy release rate and propagation direction under tensile loading (η =0^0)

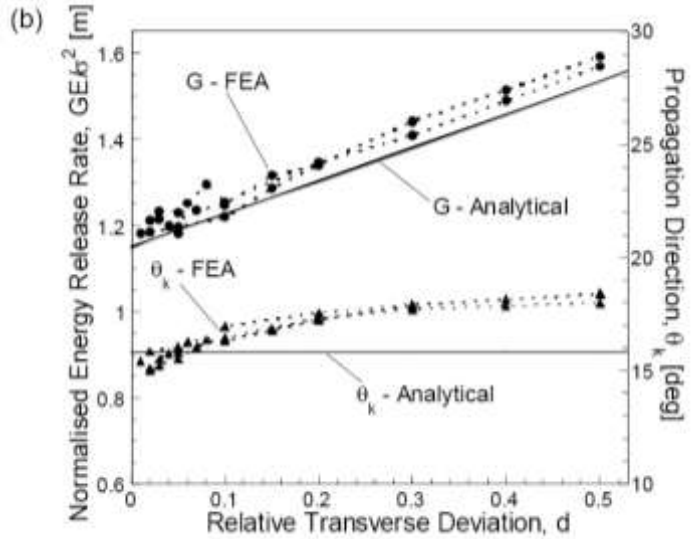

Fig. 8b Effect of transverse deviation, d, on mechanical energy release rate and propagation direction under tensile loading (η =30^0)

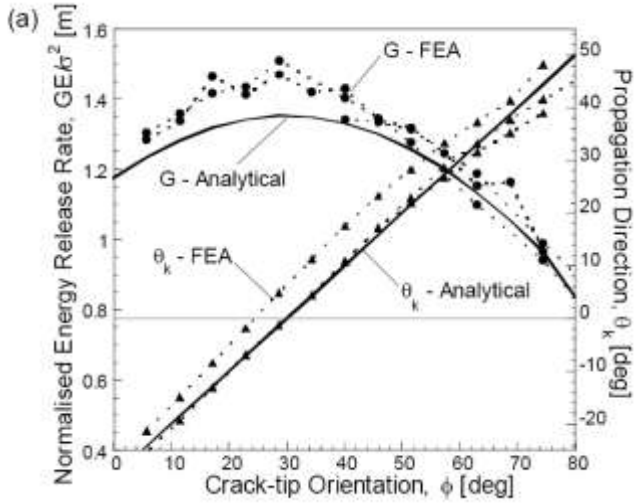

Fig. 9a Effect of crack-tip orientation on mechanical energy release rate and propagation direction under tensile loading(η =0^0)

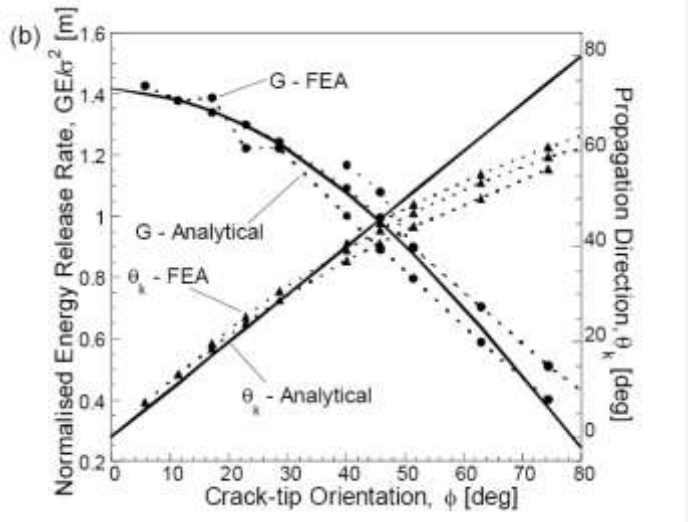

Fig. 9b Effect of crack-tip orientation on mechanical energy release rate and propagation direction under tensile loading(η =30^0)

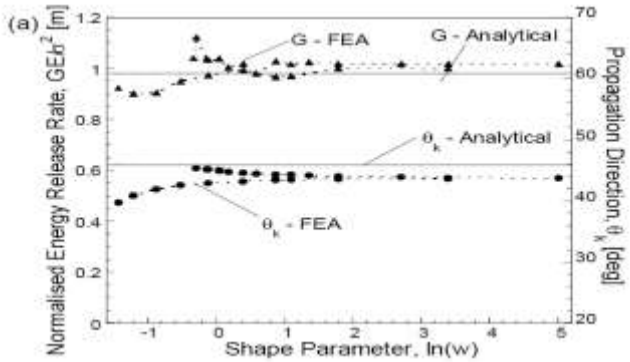

Fig 10a Effect of variation in radius of curvature at crack tip on mechanical energy release rate and propagation direction under tensile loading(η =0^0)

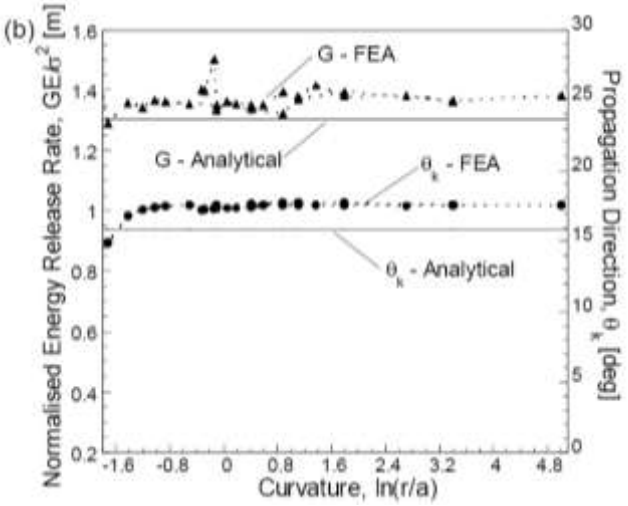

Fig 10 b Effect of variation in radius of curvature at crack tip on mechanical energy release rate and propagation direction under tensile loading(η =30^0)

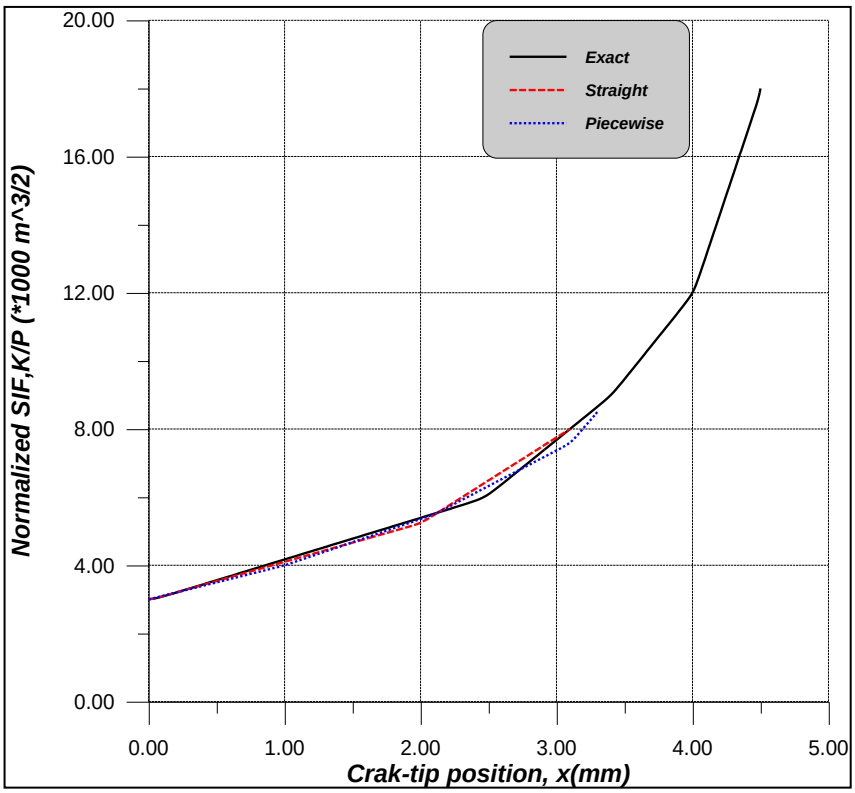

Fig. 11 Normalized stress intensity factor in homogeneous specimen for three cases of approximated cracks

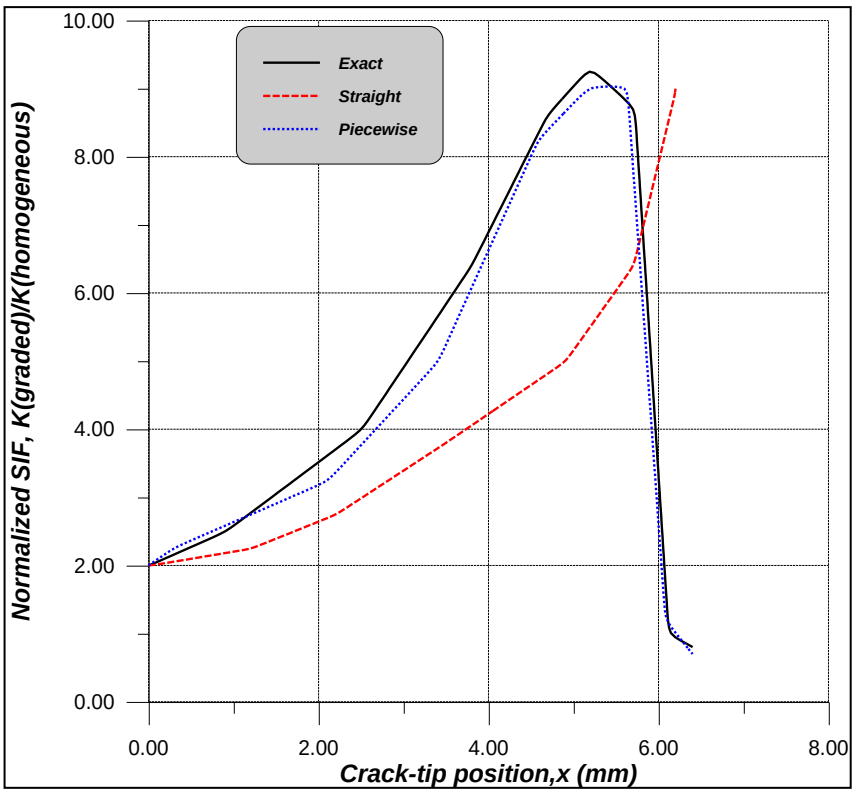

Fig. 11 Normalized stress intensity factor in bimaterial specimen for three cases of approximated cracks

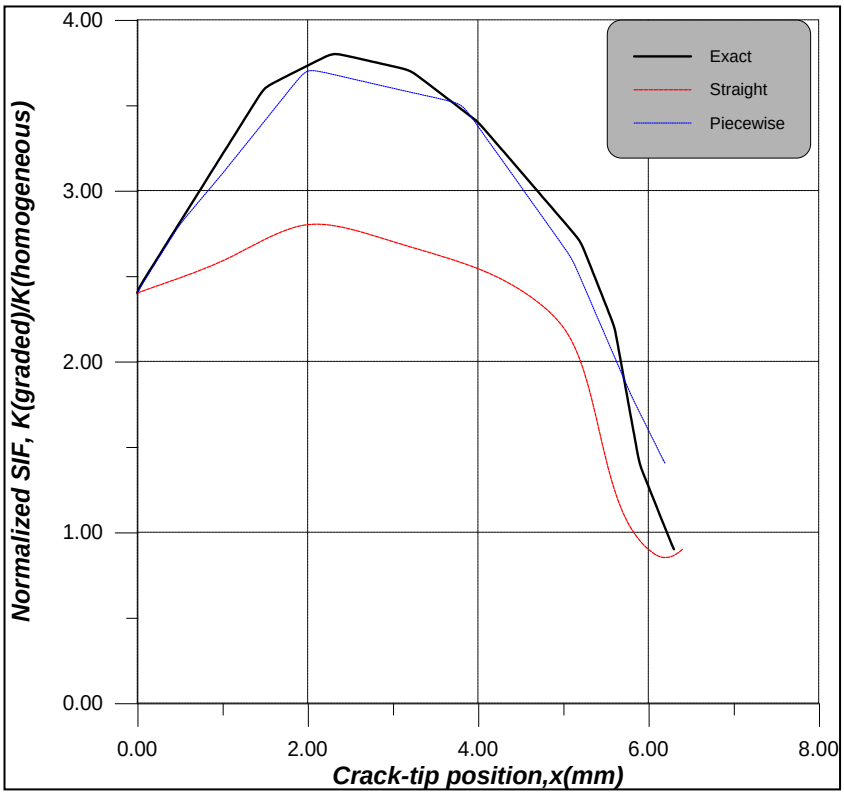

Fig. 13 Normalized stress intensity factor graded specimen(with linear variation in Young's modulus) for three cases of approximated cracks

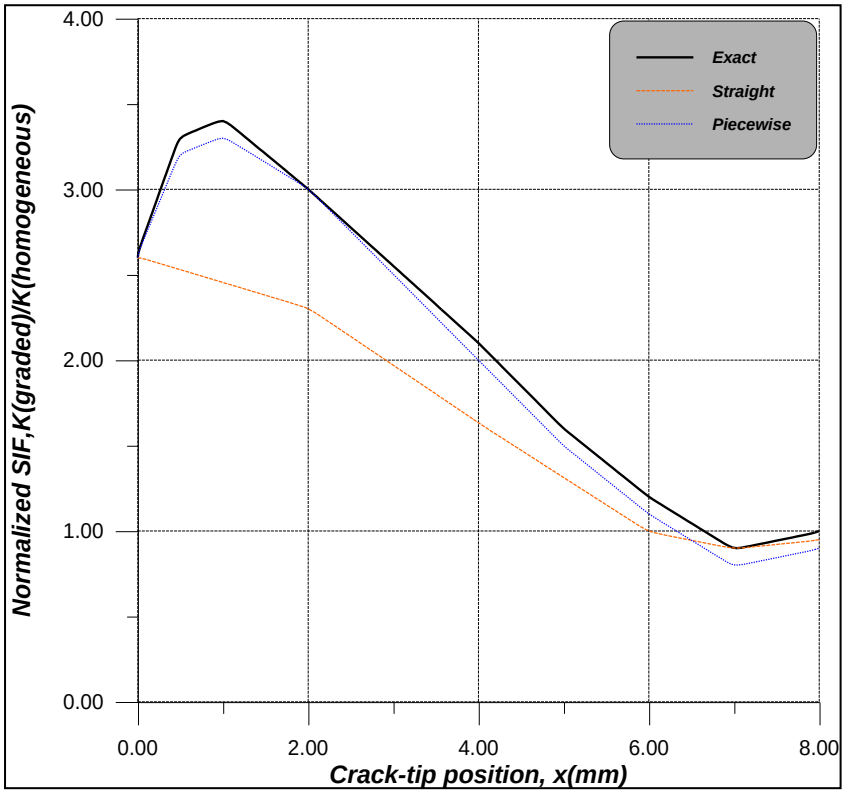

Fig. 14 Normalized stress intensity factor graded specimen(with parabolic variation in Young's modulus) for three cases of approximated cracks

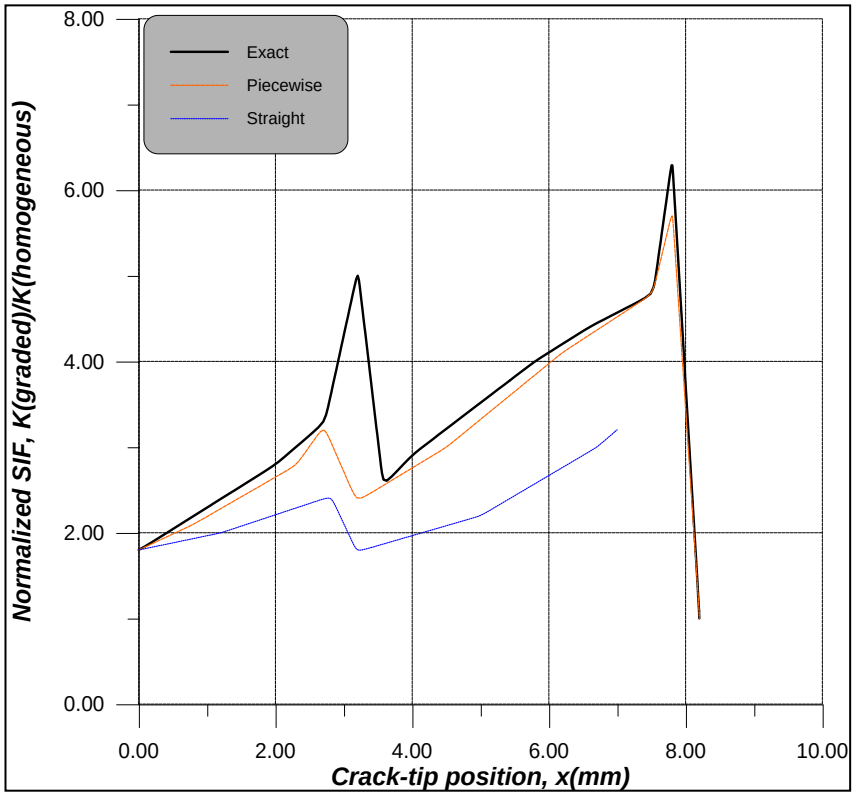

Fig. 15 Normalized stress intensity factor graded specimen (with stepped linear variation in Young's modulus) for three cases of approximated cracks

References

- ANSYS (2007) Version 11 Documentation, ANSYS Inc. Canonsburg,PA.
- Ashby MF, Jones DRH (1996), Enginering Materials 1: An introduction to their properties and applications, 2nd edition, Butterworth Heinemann.
- Broek (1991), Elementry Engineering Fructure Mechanics, 4th ed., Kluwer, Dordrecht.
- Chetterjee (2006), On The Elasic Moduli Of Some Heterogeneous, J Mech Phys Vol 13:223-227.
- Dag_, S., Kadio_lu, S. and Yahgi, O.S., 2004, "Circumferential Crack Problem for an FGM Cylinder Under Thermal Stresses", *Journal of Thermal Stresses*, Vol. 22, pp. 659-687.
- Erdogan (2006), Fracture Mechanics of FGM, Vol. 12, pp. 112-122.
- Jin, Z.-H. and Paulino, G.H., 2001, "Transient Thermal Stress Analysis of an Edge Crack in a Functionally Graded Material", *International Journal of Fracture*, Vol. 107, pp. 73-98.
- Jin & Batra(2007), Some Basic Fracture Mechanics Concepts On FGM, J Mech Phys Vol 45:20-27.
- Kitagawa H, Yurk R and Ohira T (1975) , Crack Morphological Aspects In Fracture Mechanics, Engineering Fract Mech : 515-29.
- Leevers Ps, Radon JC and Cuvler LE (1980), Fracture Trajectories In A Biaxially Stressed Plate, J Mech Phys Vol. 24: 381-390.
- Mattew T. Tllboork (2005), Thermal Fatigue Of Heterogeneous Materials, Thesis.
- Noda N, Oda K and Ishi K(1994), Analysis Of Stress Intensity Factor For Curved Cracks, JSME Int vol.6: 360-365.
- Taya , Kfouri & Khan (2005), Functionally Graded Thermal Barrier Coating, Material Science Vol. 10: 102-114.

-

List of Symbols

a: Crack length, mm
d: Transverse deviation parallel to the edge, mm
E': Effective young's modulus, Mpa
G: Mechanical energy release rate, J/mm^2
h: Height of specimen, mm
K: SIF, Mpa($\sqrt{mm}$
k: Aspect ratio of the relaxation volume
w: Gradient width, mm
$R_{E:}$ Young's modulus ratio
ϕ: Crack tip position relative to loading direction, degree
γ: Gradient parameter
η: Loading angle, degree
θ: Crack angle, degree
σ: Stress, Mpa
ξ: Relative crack position